ISSN 0018-019X

Erscheint 9mal jährlich – Paraît 9 fois par an

42. Percolative Phenomena in Microemulsions of the 'One-Component Macrofluid' Type

by **Hans-Friedrich Eicke*** and **Rolf Hilfiker**

Institute of Physical Chemistry, University of Basel, Klingelbergstrasse 80, CH–4056 Basel

and **Manfred Holz**

Institute of Physical and Electrochemistry, University of Karlsruhe, Kaiserstrasse 12, D–7500 Karlsruhe

(13.XII.83)

Summary

The temperature dependence of the water self-diffusion coefficients (D), as well as those of low- and high-field (stationary and time-dependent) specific conductivities (κ), have been determined in the percolation regime of ternary mixtures of water, AOT, and oil. For the first time a pronounced similarity in the behavior of D and κ was detected giving instructive hints about the large variations in the specific conductivities of these systems. Results from kinetic and stationary experiments are consistent with a network-structure model of microphases in the percolation regime in which the microphases retain their discrete character.

Introduction. – Being aware of the fallacy of structural models, particularly those which are used to describe multi-component systems with a predominant water or oil component, *i.e.* the so-called microemulsions, the more recently recommended self-diffusion measurements of all components of the particular system under investigation [1] seem to provide a reasonable basis for an operational definition regarding microphases and hence microemulsions. These stationary structures are then considered to be the opposite case of a molecular dispersed solution in which only random structures exist.

It might be considered a particularly favorable accident that according to the above-mentioned self-diffusion studies the extensively investigated three-component system, water, Aerosol OT and hydrocarbon, proved to be distinctly different from co-surfactant microemulsions [2]. In the former, water and surfactant self-diffusion coefficients were small, a result which reasonably suggests the structural model of microphases.

It has recently been suggested [3] that systems consisting of particles with colloidal dimensions and dispersed in a featureless medium, *i.e.* having no pairwise correlation between solvent nor between solvent and colloidal particles, should be called 'one-component macrofluids'. This view seems to us most appropriate since it emphasizes their typical feature, *i.e.* consisting of impenetrable particles [3].

To test this line of reasoning temperature-dependent self-diffusion measurements of water, specific electric conductivities at low and high fields (it was known from electro-

optic *Kerr*-effect studies that the coagulation process experienced a pronounced field-dependence [4]), and the relative viscosity of the system, were determined. These measurements and the conclusions drawn reveal interesting details which substantiate the nature of the percolation phenomenon.

Experimental. – *Chemicals.* Ternary mixtures of H_2O, Aerosol OT (sodium di-2-ethylhexylsulfosuccinate, AOT) and iso-octane (2,2,4-trimethylpentane) or hexane were prepared.

H_2O was de-ionized and doubly distilled. Hexane and iso-octane were of highest quality *(puriss.)* from *Fluka;* the solvents were distilled over CaH_2 before use. The AOT from *Fluka,* 98% of pharmaceutical quality, was purified according to the following procedure. A sufficient quantity for the experimental run (*i.e.,* 0.1 kg) was dissolved in MeOH and stirred for about 24 h in the presence of activated charcoal. The charcoal was then separated and the MeOH evaporated ($T \leqq 40°$). The remaining AOT was redissolved in 750 ml petroleum ether and the solution washed twice with 200 ml H_2O. After phase separation the petroleum-ether phase was evaporated. The gel-like residue was dissolved again in 500 ml MeOH. This solution was washed three times with 300/100/100 ml petroleum ether. The MeOH-phase was evaporated to dryness and the residue dried under vacuum. After redissolving in Et_2O the last step was repeated. The final product (AOT) was stored under Ar in a deep-freeze. The yield was 60%.

Instrumental. – i) *Self-Diffusion Measurements.* The self-diffusion coefficient measurements of H_2O in the H_2O/AOT/hexane mixture were performed using an NMR spin-echo technique (pulse magnetic field gradient (PMFG) method [5]). The pulsed spectrometer was a *Bruker B-KR 322 s* instrument working at a ^{1}H-frequency of 48 MHz. To be able to work with a simple low-resolution NMR system, 100% (D_{14})hexane was used and therefore only H_2O protons contributed to the spin-echo signal occurring at $2\tau = 80$ ms.

The pulsed magnetic field gradients were produced using a commercially available unit (*Bruker,* model *B-Z 18B*) which was combined with a home-made probe containing a quadrupole field gradient coil. Thus, we could apply magnetic field gradients in the range of 80 to 120 Gauss cm^{-1}. The duration δ of the magnetic field gradient pulses was varied between 0.5 ms and 2 ms. The pulse distance Δ (the time during which diffusion is measured) was 60 ms. To check a possible Δ-dependence of the self-diffusion coefficient which might occur under certain conditions, *e.g.* in the case of restricted diffusion [6], we also varied Δ between 5 ms and 80 ms. However, no such dependence was found.

Temperature-dependent self-diffusion coefficient measurements can be influenced by undesired convection. Therefore, we used special sample tubes, in which an inner tube, containing the liquid under investigation, is surrounded by a proton-free bath liquid (CCl_4). The bath liquid temp. was kept constant by pumping thermostated H_2O through the walls of the probe head. This experimental set-up was tested by verifying the known temperature dependence of the self-diffusion coefficient in pure H_2O.

The D-value of H_2O at 298 K in the ternary mixture was measured relative to D of pure EtOH at 298 K ($D_{EtOH} = 1.07 \cdot 10^{-9} m^2 s^{-1}$). The water self-diffusion coefficients at the different temperatures were then measured relative to the value at 298 K.

ii) *Electrical Conductivity Measurements. Wayne-Kerr*-bridge *B 221* was used with a measuring frequency of 1592 Hz. This instrument is in principle a *Wheatstone* bridge with resistance and capacitance balances. The cell was equipped with Pt-electrodes at constant distance.

iii) *Electrical Conductivity Measurements at High (ac) Field which was Applied Perpendicular to the Measuring Direction (Fig. 1).* The high-voltage electrodes were separated by insulating layers from the solution to

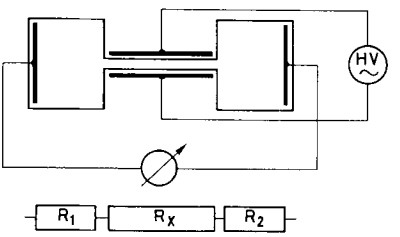

Fig. 1. *Scheme of electrolytic cell with measuring and high-voltage (HV) electrodes.* R_1, R_x, and R_2 are the resistances of the corresponding three compartments as shown in the scheme. For details see text.

prevent any current flow. The cell construction should fulfill two conditions. *i*) Disturbing effects of the electric field on the conductivity measurements should be minimized. *ii*) Changes of the physical state of the solution produced by the electric field should exert the greatest possible effect on the measured resistance.

Disturbance of the conductivity measurements by the electric field was minimized by choosing a large distance between high-voltage and measuring electrodes. Moreover, the high-voltage was allowed to float with respect to ground, while the measuring electrodes were kept at almost ground potential which again reduced the influence of possible stray fields on the latter. Accordingly, the electrolytic cell can be considered as consisting of three resistors in series, R_1, R_x and R_2 where only the middle one, R_x, is influenced by the high field. Since at low field conductance R_x is about twenty times ($R_1 + R_2$), the total resistance is essentially determined by R_x. Also, stray fields which form at the rim of the high-voltage electrodes affect only R_1 and R_2 (for geometric reasons); the effects of these, however, are much smaller than the measured conductivity and can reasonably be neglected. The specifications of the high-voltage generator were, 14.5 kHz sinusoidal floating voltage, $U_0 \approx 3$ kV, and effective field strength, *ca.* $9 \cdot 10^5$ V m^{-1}. The hermetically sealed measuring cell could be thermostated by immersing it in a temperature bath.

iv) *Viscosity measurements* were performed at various temperatures with an *Ubbelode* viscometer. From the temperature-dependent viscosities of the mixture and the continuous oil phase the temperature-dependent relative viscosity was derived.

Results and Discussion. – Several authors have already reported [7–9] more or less marked increases in the electric conductivity with either increased temperature or volume fractions of water (in oil-continuous systems); however, in each case they used at least four components, *i.e.* 'co-surfactant microemulsions'. We consider it an essential advantage that the above-mentioned phenomenon of the quasi-sudden increase of the conductivity can be nicely studied in a three-component system. To the best of our knowledge it is the first time that, parallel to the increase in the electric conductivity, a quasi-sudden increase of the water self-diffusion coefficient is observed. *Fig. 2* presents temperature-dependent self-diffusion coefficients of water, low-field specific conductivity and relative viscosities of a water/AOT/(D_{14})hexane mixture with [H_2O]/[AOT] = 46.2 and c_{AOT} = 0.163 mol dm^{-3}. The plot demonstrates different temperature-dependent changes of the physical properties of the system, phenomenologically described by the degree of co-operativity. The latter is most pronounced for the specific conductivity, and lesser for the self-diffusion coefficients and the relative viscosities. In connection with these observations it should be mentioned that, owing to the well-known relationship between diffusion coefficient and viscosity, the simultaneous in-

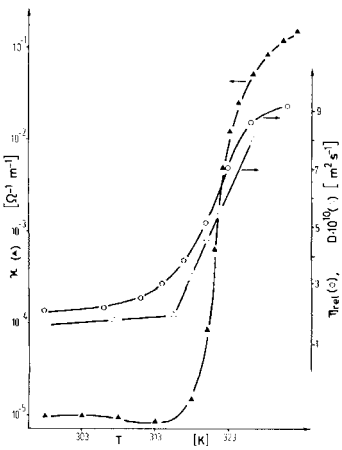

Fig. 2. *Relative viscosity, self-diffusion coefficients of water, and the logarithm of the specific conductivity* vs. *temperature.* System: H_2O/0.163 mol dm^{-3} Aerosol OT/hexane ((D_{14})hexane); [H_2O]/[AOT] = 46.2.

crease of both quantities clearly relates them to different physical processes. The temperature dependence of the viscosity is attributed to the increasing clustering of the microphases and the corresponding change of the macroscopically determined viscosity. This, initially local, clustering is expected to end with a macro-cluster (with further increase in temperature), *i.e.* a network-like assembly of microphases, which is the prerequisite for the onset of a considerable water diffusion expressed by the water self-diffusion coefficient.

Temperature-dependent viscosities and electro-optic *Kerr*-effect measurements of ternary water/AOT/hydrocarbon mixtures yielded the first indication regarding the above mentioned network formation of microphases [10]. Two remarkable observations are displayed in *Fig. 2:* the relatively large variations of the absolute values of the specific conductivity and of the self-diffusion coefficients and the large activation energies of the underlying processes. These results hint at a network structure formation of the aqueous microphases. Of particular interest is the activation energy of the temperature-dependent self-diffusion coefficients which is in accord with theoretical estimates and other experimental data.

An *Arrhenius* plot of the self-diffusion coefficients of water (see *Fig. 3*) displays two distinct branches. The low-temperature branch yields a rather small activation energy. It corresponds to the low-concentration realm with predominantly individual microphases which undergo frequent collisions with occasional diffusion-controlled water exchange [11]. The absolute value of the water self-diffusion coefficient supports this water-exchange mechanism: it can be seen from the absolute value of the mean square displacement $< r^2 >$. We can calculate from $< r^2 > = 2\,D\,t$ the average displacement $< r > = \sqrt{< r^2 >}$ in the direction of the magnetic field gradient. With $D = 1.67 \cdot 10^{-10}$ $m^2\ s^{-1}$ at 298 K and with $t = 1$ s, we arrive, for example, at $< r > = 1.8 \cdot 10^{-5}$ m, a value which corresponds to about 900 diameters of individual microphases per second. Since from photon-correlation spectroscopy and ultracentrifugation (sedimentation) studies [12] one obtains coinciding displacements of microphases of 450 diameters per second in one direction, there exists a significant hint to a water-exchange mechanism between individual microphases.

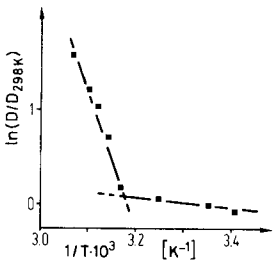

Fig. 3. Arrhenius *plot of self-diffusion coefficients of water in mixture of* H_2O, 0.163 mol dm^{-3} Aerosol OT, (D_{14})hexane, $[H_2O]/[AOT] = 46.2$.

The intersection of the two branches denotes, according to our structural model concept, the onset of a network formation. The large activation energy of the H_2O-self-diffusion coefficients (*ca.* 120 kJ mol^{-1}) compared with that in pure water (19 kJ mol^{-1}) excludes any model with a coherent water structure. Also, the assumption of a critical

molecular dispersed mixture of water, AOT and oil appears incompatible with this result.

If we adopt the above-mentioned (three-dimensional) network-structure model where each microphase preserves its individuality, the water molecule is forced to diffuse through some kind of bilayer structure if a transport process of water is considered. The total activation energy of the water diffusion in these systems can be split into three contributions: *i*) abstraction of a water molecule from the bulk-like water in the microphase, *i.e.* the molecular evaporation enthalpy, $\Delta_f^g h$, *ii*) the molecular free energy for creation of a spherical, oil/water interface in the oil continuum, $\Delta f = 4\pi r^2 \gamma_{o/w}$ with $r = 1.9 \cdot 10^{-10}$m ($\approx$ radius of water molecule) and $\gamma_{o/w}$ (interfacial free energy of oil/water interface) $= 5.1 \cdot 10^{-2}$ Nm^{-1}, and *iii*) the polarization energy necessary to polarize the oil by the water dipole $(\mu_{H_2O}), w_{pol} = [(\varepsilon_{oil}-1)/(\varepsilon_{oil}+2)]\{1/4\pi\varepsilon_0\}\mu_{H_2O}^2/r^3$ with $\mu_{H_2O} = 6.17 \cdot 10^{-30}$ As m, $\varepsilon_{oil} = 1.9$ (typical dielectric constant of aliphatic hydrocarbon at 293 K) and ε_0 the permittivity of vacuum. The overall contribution to the energy of activation per mole of the self-diffusion is then calculated to be approximately 66 kJ mol^{-1}. This result agrees reasonably well with experimental data obtained by *Prince & Thompson* [13] for water diffusion through lipid membranes who determined an activation energy between 52 and 58 kJ mol^{-1}.

The above-mentioned value of the activation energy of the water-diffusion process is considerably larger than this calculated and experimentally confirmed value. It does not seem unreasonable, therefore, to assume that the value 120 kJ mol^{-1} is made up of at least two contributions. Since the proposed network-structure (ns) formation is accompanied by an enthalpy of seggregation $\Delta_{sol}^{ns} H$ it is possible to consider this as the second contribution to the overall activation energy. Additional evidence regarding such a second contribution will be presented below.

The magnitude of this seggregation enthalpy can be qualitatively estimated from the field-induced shift of the critical point describing a transition between sol and extended network structure of microphases [10]. This enthalpy can only be estimated rather qualitatively to be of the same order of magnitude as the above calculated energy contribution of the diffusion process if some aggregation of the microphases is assumed. The latter corresponds to the excess enthalpy of mixing of the microphases and the dispersion medium.

Apart from these self-diffusion measurements which strongly point to structure formation in these systems under specific conditions, electro-optic *Kerr* effect [4], permittivity [14] and small angle light-scattering studies [15] demonstrate convincingly the approach to a critical point.

Low- and High-Field Specific Conductivity. The most popular transport phenomenon used for investigating the percolation is the electric conductivity (κ). As already mentioned in the context of and exhibited in *Fig. 2*, the conductivity plot resembles that of the self-diffusion coefficient although, it indicates a more pronounced cooperativity. Apparently, the conductivity is more sensitive towards network-structure formation.

Below the so-called percolation temperature (extrapolated temperature at which the onset of percolation is assumed) the specific conductivities are of the order of 10^{-6} to 10^{-5} Ω^{-1} m^{-1}. It is reasonable to assume (and supported by experiment [16]) that in this temperature region aqueous microphases exchange charges during their frequent collisions. The considerable increase of κ, however, in approaching the percolation regime

cannot be explained by this model. Even if all the microphases were singly charged, the electric conductivity of a (water/0.14 mol dm^{-3} AOT/iso-octane)-solution with $[H_2O]/[AOT] = 65$ would amount to about $3 \cdot 10^{-4}\ \Omega^{-1}\ m^{-1}$. Actually, conductivities up to $10^{-2}\ \Omega^{-1}\ m^{-1}$ were measured.

Accepting that the network structure is dominant in the percolation region and that this structure consists of individual, mutually connected, microphases according to the above discussion of self-diffusion measurements, a charge separation and, hence, an electric conductivity is conceivable by rotating a surfactant anion (in the case of AOT) from one microphase to another. Each surfactant molecule could be involved in such a process. Thus, there exists a high probability for such a charge separation and (isotropic) conductivity. The activation energy for a single event should be not too high for two reasons: *i*) the rotating anion is hydrated which can be shown to reduce the activation energy for charge transport [17], and *ii*) the charge separation process avoids direct oil contact by displacing the charge within the 'lamellar' structure of the microphase network (as might be easily visualized). Moreover, owing to the high (local) concentration of potential charge carriers, the frequency factor for this conduction process is expected to be large and hence a considerable conductivity is to be expected. This qualitative model elucidates the difference regarding self-diffusion and electric conductivity. The conductivity should be more structure-sensitive than the diffusion process.

Thus the total specific conductivity (κ) is composed of two contributions, *i.e.*

$$\kappa = (\Lambda_{sol}\,[M_{sol}] + \Lambda_{ns}\,[M_{ns}])\ 10^3 \tag{1}$$

where Λ_{sol} is the molar conductivity due to momomeric or oligomeric microphases or microphase clusters dispersed in the continuous oil phase, and Λ_{ns} is the molar conductivity due to the network structure of mutually interconnected microphases. $[M_{sol}]$ and $[M_{ns}]$ are the corresponding concentrations. Since $\Lambda_{ns} \gg \Lambda_{sol}$, κ is essentially determined by $\Lambda_{ns}[M_{ns}]$ in the percolation regime. Structure formation is favored by increasing temperature, hence the enthalpy ($\Delta^{ns}_{sol}H$) and entropy ($\Delta^{ns}_{sol}S$) of seggregation must be positive. The positive value of the enthalpy ensures a shift of the equilibrium with increasing temperature towards a (continuous) network-structure formation. $\Delta^{ns}_{sol}S > 0$ warrants $\Delta^{ns}_{sol}G < 0$, *i.e.* network-structure formation is a spontaneous process. A molecular interpretation of the positive entropy has to consider the desolvation of oil molecules from the microphases during network formation.

A straightforward approach for thermodynamically describing network-structure formation is to assume an equilibrium between microphases in the monomeric or oligomeric sol- and network-structure states, *i.e.*

$$M_{sol} \rightleftarrows M_{ns} \tag{2}$$

with

$$K = [M_{ns}]/[M_{sol}]. \tag{2a}$$

The temperature dependence of this equilibrium is predicted by *van't Hoff*'s law, *i.e.* $d\ln K/dT = \Delta^{ns}_{sol}H/RT^2$ which can be integrated with respect to T if $\Delta^{ns}_{sol}H$ is taken to be

temperature-independent within a certain temperature interval. The latter is a reasonable assumption in view of the physical situation. Hence,

$$K(T) = K(T_o) \exp\{(\Delta^{ns}_{sol}H/R)\,(1/T_o - 1/T)\}, \tag{3}$$

where T_o is a reference temperature related to the sol-state of the microphases.

From *Eqn. 2a* we obtain

$$[M_{ns}] = K\,[M_{sol}]. \tag{2b}$$

Introducing the conservation of mass $[M_{ns}] + [M_{sol}] = c_o$ into *Eqn. 2b* yields

$$[M_{ns}] = \frac{K}{1 + K}\,c_o \tag{4}$$

which can be modified by inserting *Eqn. 3* into *Eqn. 4* in order to describe the temperature-dependent network-structure formation (ns). Thus

$$[M_{ns}] = \frac{K(T_o) \exp\{(\Delta^{ns}_{sol}H/R)\,(1/T_o - 1/T)\}}{1 + K(T_o) \exp\{(\Delta^{ns}_{sol}H/R)\,(1/T_o - 1/T)\}}\,c_o. \tag{5}$$

A plot *(Fig. 4)* of the microphase concentration within the network structure *vs.* the temperature according to *Eqn. 5* shows a pronounced cooperative behavior.

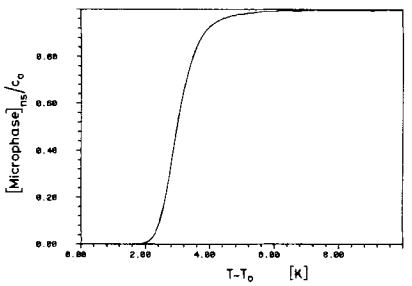

Fig. 4. *Microphase concentration in the network-structure regime* (ns) *normalized with respect to total concentration of microphase* (c_o) vs. *temperature*

Let E_κ be the activation energy of the conduction process in the network structure (ns), then

$$\Lambda_{ns} = \Lambda^0_{ns} \exp(-E_\kappa/RT) \tag{6}$$

or

$$\kappa_{ns} = \Lambda^0_{ns}\,[M_{ns}] \exp(-E_\kappa/RT) \cdot 10^3. \tag{6a}$$

According to the above remark regarding the overall conductivity, κ is essentially equal to κ_{ns} within the percolation regime. We thus obtain by combining *Eqn. 5* and *6a*

$$\kappa(T) \simeq \Lambda^0_{ns}\, c_o\, 10^3 \frac{K(T_o) \exp\{(\Delta^{ns}_{sol}H/R)\,(1/T_o - 1/T)\}}{1 + K(T_o) \exp\{(\Delta^{ns}_{sol}H/R)\,(1/T_o - 1/T)\}}\, e^{-E_\kappa/RT}. \qquad (7)$$

An interesting approach for obtaining details of the conduction process within the percolation regime is offered by the application of high electric fields (*via* insulated electrodes) perpendicular of the measuring electrodes. The promoting effect of the electric field on the network-structure formation has been already observed with electro-optic *Kerr*-effect investigations. In the present case stationary and time-dependent experiments provide particular information on the network-structure formation and on charge generation, recombination and conduction mechanism. It is relevant in this connection to study the relative increase of the specific conductivity $\kappa(t = \infty)/\kappa(t = 0) - 1$ under high applied field (*Fig. 5*). An asymmetric distribution of the 'relative excess conductivity' is obtained, *i.e.* there exists a particular temperature, T_{max}, where the effect of the electric field on the conductivity is maximal.

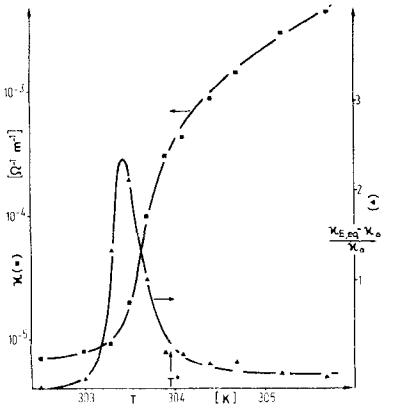

Fig. 5. *Specific* (■) *and relative excess* (▲) *conductivities* vs. *temperature*. System: H_2O/0.138 mol dm^{-3} Aerosol OT/i-octane; $[H_2O]/[AOT] = 55$.

As already mentioned the electric field favors the formation of the network structure which does not appear unreasonable in view of the induced dipole interactions. Hence, it is to be expected that the enthalpy of formation of the network structure decreases under the influence of the field. Simultaneously, the activation energy for the charge separation should decrease due to the high field (*Wien* effect) and, hence, enhance the electric conductivity. The plot of relative excess conductivity may then be interpreted as being strongly determined by the field-induced network-structure formation of microphases yielding the steep increase of the excess conductivity. As soon as the structure formation is complete, the conductivity drops to the value predicted by *Onsager*'s theory of the *Wien* effect. This concept will be confirmed by time-dependent studies of the conductivity to be described below.

The field-dependent conductivity can be described analogously to *Eqn. 7, i.e.*

$$\kappa(E,T) = \Lambda^0_{ns}\, c_o\, 10^3 \frac{K(T_o,E) \exp\{(\Delta^{ns}_{sol}H(E)/R)\,(1/T_o - 1/T)\}}{1 + K(T_o,E) \exp\{(\Delta^{ns}_{sol}H(E)/R)\,(1/T_o - 1/T)\}}\, e^{-E_\kappa(E)/RT} \qquad (8)$$

where $\Delta^{ns}_{sol}H(E) < \Delta^{ns}_{sol}(E = 0)$ and $E_\kappa(E) < E_\kappa(E = 0)$. The relative excess conductivity is defined by

$$\frac{\kappa(E) - \kappa(E=0)}{\kappa(E=0)}. \tag{9}$$

A plot of the relative excess conductivities utilizing *Eqn. 7* and *8* for three different values of $\Delta^{ns}_{sol}H(E)$ is exhibited in *Fig. 6*. The apparent dissymmetry of the curves is due to the difference of $E_\kappa(E)$ and $E_\kappa(E = 0)$. The similarity between experimental *(Fig. 5)* and the theoretical plots is apparent and might be considered also to support the underlying model.

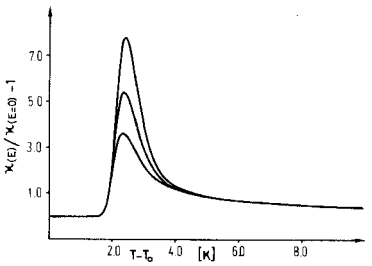

Fig. 6. *Theoretical plot according to* Eqn. 9 vs. *temperature for three different values of* $\Delta^{ns}_{sol}H$ (see text)

Apart from the above described stationary measurements, kinetic experiments have been carried out by following the temporal change of the conductivity after switching the high field on or off. Temporal rise and decay of the conductivity could be well-fitted only with a second-order rate law: $d\kappa/dt = k\{\kappa(t = \infty) - \kappa\}^2$. For a comparison of rate constants at different temperatures, a normalized rate constant (k_{rel}) proved physically more realistic than k derived from this equation. This normalization was done in such a way that the normalized conductivity varied only between 0 and 1.

Temperature Dependence of Normalized Rate Constants. Fig. 7 shows the logarithms of the normalized rate constants for rise and decay of the conductivity plotted *vs.* the

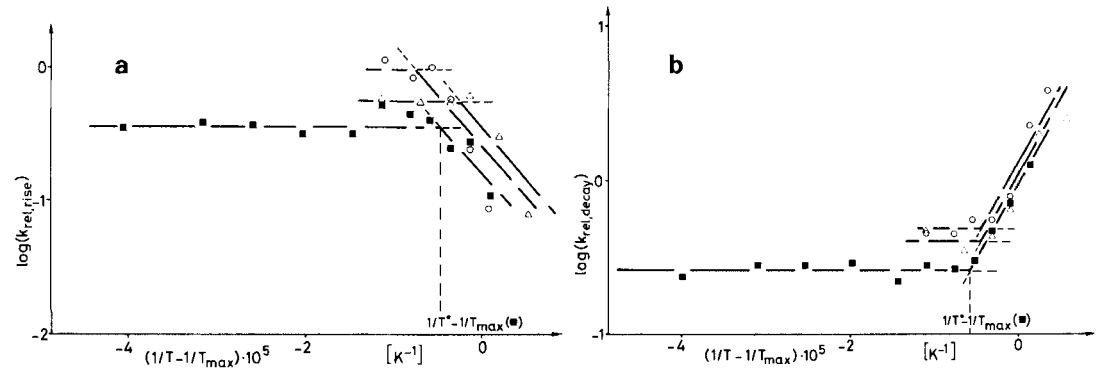

Fig. 7. Arrhenius *plots of rate constants for rise* (a) *and decay* (b) *of conductivities after applying and turning off the high electric field.* System: H_2O/Aerosol OT/i-octane; c_{AOT}: 0.109 mol dm^{-3}, [H_2O]/[AOT] = 65 (○); c_{AOT}: 0.138 mol dm^{-3}, [H_2O]/[AOT] = 65 (△); c_{AOT}: 0.138 mol dm^{-3}, [H_2O]/[AOT] = 55 (■).

difference of the inverse temperatures, $(1/T-1/T_{max})$, the second term in the bracket refers to the temperature where the maximum of the relative excess conductivity occurs. The plot *(Fig. 7a)* consists of two branches: the energy of activation is almost zero for $T > T^*$ and positive for $T < T^*$. The corresponding plot *(Fig. 7b)* exhibits the same feature of the activation energy for $T > T^*$, however, a negative value for $T < T^*$. The logarithms of the ratio $k_{rel,decay}/k_{rel,rise}$ against $1/T-1/T_{max}$ is shown in *Fig. 8* for two different volume fractions of water in the water/AOT/iso-octane mixture at 0.138 mol dm^{-3} AOT.

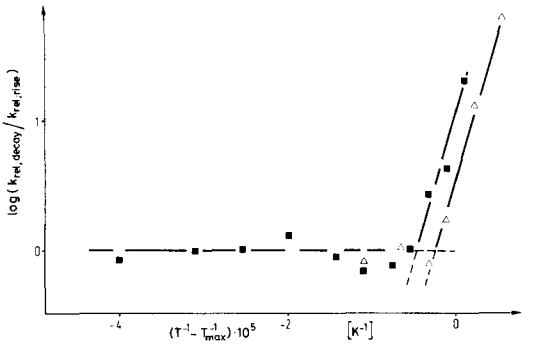

Fig. 8. *Ratio of rate constants for rise and decay of conductivities.* System and notation as in *Fig. 7.*

Fig. 7a,b demonstrate that at a particular temperature, T^*, apparently a change of mechanism occurs. A comparison with *Fig. 5* reveals that this temperature coincides approximately with the inflection point of the $\kappa(T)$-plot, probably indicating a termination of the network-structure formation of microphases.

It is possible to suggest a kinetic model which readily explains the experimentally observed temperature dependence of the rate constants: *i)* rise of conductivity (high-field applied)

$$2\ M_{sol} \underset{k_{-1}}{\overset{k_1}{\rightleftarrows}} 2\ M_{ns} \overset{k_2}{\rightarrow} M_{ns}^+ + M_{ns}^- \tag{10}$$

where M denotes a microphase, subscript 'sol' and 'ns' refer to the free and network states of the microphases, respectively. We further assume that the equilibrium constant K_1 is related to an enthalpy of network-structure formation, $\Delta_{sol}^{ns}H$, the rate constant k_2 to an activation energy E_a. Within the temperature region $T < T^*$ where the network-structure (ns) is being formed, we apply the steady state condition, *i.e.*

$$\frac{d[M_{ns}]}{dt} = 2\ k_1[M_{sol}]^2 - 2\ k_{-1}[M_{ns}]^2 - 2\ k_2[M_{ns}]^2 = 0 \tag{11}$$

from which $[M_{ns}]$ is obtained, *i.e.*

$$[M_{ns}] = (k_1/(k_{-1} + k_2))^{1/2}\ [M_{sol}]. \tag{12}$$

The observed conductivity within the network-structure-forming region is attributed formally to species of the kind M_{ns}^+ and M_{ns}^-, hence $\kappa = \text{const}\,[M_{ns}^+]$, or

$$\frac{d\kappa}{dt} = \text{const}\,\frac{d[M_{ns}^+]}{dt} = \text{const}\,k_2\,[M_{ns}]^2. \tag{13}$$

This relation is combined with *Eqn. 12* which relates the temporal change of the conductivity with the concentration of microphases in the sol-state.

$$\frac{d\kappa}{dt} = \text{const}\,\frac{k_1 k_2}{k_{-1} + k_2}\,[M_{sol}]^2. \tag{14}$$

The overall rate constant is

$$k^\dagger = \frac{k_1 k_2}{k_{-1} + k_2}. \tag{14a}$$

It will be shown later that $k_{-1} > k_2$, hence

$$k^\dagger \simeq \frac{k_1}{k_{-1}}\,k_2 = K_1\,k_2. \tag{15}$$

The energy of activation $E_a^\dagger$ is then given by (see *Eqn. 10*)

$$E_a^\dagger = RT^2\left(\frac{d\ln K_1}{dT} + \frac{d\ln k_2}{dT}\right) = \Delta_{sol}^{ns}H + E_a \tag{16}$$

The experimentally observed energy of activation is > 0.

Within the temperature region where the network formation is almost complete, we have from *Eqn. 10* for the dissociation process

$$2\,M_{ns} \overset{k_2}{\rightarrow} M_{ns}^+ + M_{ns}^-. \tag{10a}$$

Then, $k_2 = k^\dagger$ and accordingly $E_a = E_a^\dagger$. The observed energy of activation is approximately zero, *i.e.* since $E_a + \Delta_{sol}^{ns}H > 0$ and $E_a \simeq 0$, $\Delta_{sol}^{ns}H > 0$. The enthalpy of formation of the network is positive.

ii) Conductivity decay: the charge recombination can be described by

$$M_{ns}^+ + M_{ns}^- \underset{k_{-3}}{\overset{k_3}{\rightleftarrows}} M_{sol}^+ + M_{sol}^- \overset{k_4}{\rightarrow} 2\,M_{sol} \tag{17}$$

and

$$M_{ns}^+ + M_{ns}^- \overset{k_{-2}}{\rightarrow} 2\,M_{ns} \tag{17a}$$

where the first process simulates the charge recombination for incomplete network-structure formation, while the second is valid for completed network-structure. It should be noted that the reverse mechanism to *Eqn. 10* would not be suitable to inter-

pret the experimentally observed temperature dependence of the rate constant. Hence, it has to be concluded that in the region of incomplete network-structure formation the charge recombination is slower than the decomposition rate of the network structure. This assumption was already made in the previous paragraph (*i*). Analogous considerations as in (*i*) yield:

$$E_a^{\dagger} = E_a + \Delta_{ns}^{sol}H < 0 \quad \text{for} \quad T < T^* \quad \text{and} \quad E_a^{\dagger} \approx E_a \approx 0 \quad \text{for} \quad T > T^*.$$

Consistent with the considerations under (*i*) the excess mixing enthalpy of the microphases in the continuous oil phase is negative. Finally, it is seen from *Fig. 8* that the rate of the charge production and recombination is about equal.

In summary, the above results and discussions do not support a coherent water structure over macroscopic distances, an argument which was occasionally put forward for multi-component microemulsions. Instead, it appears that the results substantiate again the individuality of the microphases up to the lower consolute point of the system.

The authors wish to thank Prof. *H.G. Hertz* for his interest in this work. The latter is part of the project No. 2.527-0.82 of the *Swiss National Science Foundation (H.-F.E.)* and project No. H0.805/3-2 of the *Deutsche Forschungsgemeinschaft (M.H.)*.

REFERENCES

[1] *B. Lindman, P. Stilbs & M.E. Moseley*, J. Colloid Interface Sci. *83*, 569 (1981).
[2] *P. Stilbs & B. Lindman*, J. Colloid Interface Sci., in press.
[3] *J.B. Hayter*, Faraday Disc. No. 76 (1983).
[4] *H.F. Eicke & D. Dünnenberger*, in preparation.
[5] *E.O. Stejskal & J.E. Tanner*, J. Chem. Phys. *42*, 288 (1965).
[6] *J.E. Tanner & E.O. Stejskal*, J. Chem. Phys. *49*, 1768 (1968).
[7] *M. Lagües & C. Sauterey*, J. Phys. Chem. *84*, 3503 (1980).
[8] *M. Lagües*, J. Phys. Lett. *40*, L-331 (1979).
[9] *A.M. Cazabat, D. Chatenay, J. Meunier & A. Pouchelon*, J. Phys. Lett. *43*, L-89 (1982); *A.M. Cazabat, D. Chatenay, P. Guering, D. Langevin, J. Meunier, O. Sorba, J. Lang, R. Zana & M. Paillette*, Proc. Int. Symp. Surfactants in Solut., Lund; Plenum Publ. Corp., New York, 1983.
[10] *H.F. Eicke & R. Kubik*, Faraday Disc. No. 76 (1983).
[11] *H.F. Eicke, J. Shepherd & A. Steinemann*, J. Colloid Interface Sci. *56*, 168 (1976).
[12] *M. Zulauf & H.F. Eicke*, J. Phys. Chem. *83*, 480 (1979).
[13] *H.D. Prince & T.E. Thompson*, J. Mol Biol. *41*, 443 (1969).
[14] *S. Geiger*, unpublished results, Inst. of Physical Chem. Univ. of Basel, 1983.
[15] *G. Furler*, Ph.D. thesis, Univ. of Basel, 1983.
[16] *H.F. Eicke & A. Denss*, Solution Chemistry of Surfactants, Vol. 2, Plenum Publ. Corp., New York, 1979, p. 699.
[17] *R.C. MacDonald*, Bioch. Biophys. A *448*, 193 (1976).